



CHALMERS
UNIVERSITY OF TECHNOLOGY

Corrosion of Austenitic Stainless Steel Welds in Chloride Containing Environments

Master's Thesis in Materials Engineering

JOSH TURAN

Department of Chemistry and Chemical Engineering

CHALMERS UNIVERSITY OF TECHNOLOGY

Gothenburg, Sweden 2018

MASTER'S THESIS 2018

**Corrosion of Austenitic Stainless Steel Welds in
Chloride Containing Environments**

JOSH TURAN



CHALMERS
UNIVERSITY OF TECHNOLOGY

Department of Chemistry and Chemical Engineering

CHALMERS UNIVERSITY OF TECHNOLOGY

Gothenburg, Sweden 2018

Corrosion of Austenitic Stainless Steel Welds in Chloride Containing
Environments

JOSH TURAN

© JOSH TURAN, 2018.

Supervisor: Annika Zieseniss, Volvo Car Group

Examiner: Jan-Erik Svensson, Chemistry and Chemical Engineering, Chalmers Uni-
versity of Technology

Master's Thesis 2018

Department of Chemistry and Chemical Engineering

Chalmers University of Technology

SE-412 96 Gothenburg

Telephone +46 31 772 1000

Corrosion of Austenitic Stainless Steel Welds in Chloride Containing Environments

Josh Turan

Department of Chemistry and Chemical Engineering

Chalmers University of Technology

Abstract

This thesis work focuses on the corrosion behaviour of austenitic stainless steel welds in chloride containing environments. The initial aim was to develop a new method for corrosion testing of welded austenitic stainless steel. The motivation for such work was that previous results indicated that the current accelerated corrosion tests are too harsh for these welds. The specific application is for a stainless steel automotive fuel tank that is being investigated as a possible alternative to the standard plastic fuel tank. For this study, lab-welded samples of 304L and 301 stainless steel were provided by Outokumpu for accelerated corrosion testing. The corrosion mechanisms of most concern were stress corrosion cracking and intergranular corrosion.

Three different accelerated corrosion test (ACT) cycles were used. These included two standard Volvo Cars cycles and one new experimental cycle. Chloride environments containing NaCl and a mixture of NaCl and CaCl₂ were included. Lastly, an ASTM standard for stress corrosion cracking of stainless steel was utilized. Results showed that the lab-welded samples were corrosion resistant under all conditions due to excellent weld quality. The two different chloride environments did not show significant differences in corrosive attack.

Keywords: Stress Corrosion Cracking, Intergranular Corrosion, Stainless Steel

Acknowledgements

I would like to acknowledge and thank those who helped me along the way with this thesis work. First and foremost, my supervisor Annika Zieseniss at Volvo Cars for guiding me along this project. Also, thanks to Adeline Flogård and Mats Ström for their input and advice. Lastly, thanks to Stefan Schubert from Outokumpu for his support and collaboration on this project.

Josh Turan, Gothenburg, July 2018



Contents

List of Figures	xi
1 Introduction	1
1.1 Stainless Steel Fuel Tank	1
1.2 Scope of Work	3
1.3 Austenitic Stainless Steel	3
1.4 Influence of Alloying Elements on Corrosion Resistance	4
1.5 Corrosion of Steels	6
1.6 Corrosion Mechanisms	8
1.6.1 Pitting Corrosion	8
1.6.2 Stress Corrosion Cracking (SCC)	9
1.6.3 Intergranular Corrosion	11
1.7 The Effect of Welding on Corrosion	13
1.8 The Role of Ferrite Content	14
2 Materials and Methods	17
2.1 Artificial Mud	18
2.2 Climate Chamber Tests	19
2.3 ACT 1	21
2.4 ACT 2	22
2.5 EXP 1	24
2.6 ASTM Test for Stress Corrosion Cracking	24
3 Results and Discussion	27
3.1 Laboratory Climate Chamber Tests	27

Contents

3.1.1	ACT 1	27
3.1.1.1	Lab-welded Samples	27
3.1.2	ACT 2	29
3.1.2.1	Lab-welded Samples	29
3.1.3	EXP 1	30
3.2	ASTM Stress Corrosion Cracking	32
4	Conclusion	35
5	Outlook	37
	Bibliography	39

List of Figures

1.1	Coupled electrochemical reactions occurring at different sites on the same metal surface for iron in a neutral or basic solution	7
1.2	Time-temperature-sensitization curves for type 304 stainless steel in a mixture of CuSO_4 and HSO_4 containing copper. Source: Ref 14. Curves A and B indicate high and medium cooling rates, respectively	12
1.3	Shaeffler diagram for estimating steel microstructure	15
2.1	Chemical compositions of stainless steels 301 and 304L.	17
2.2	Split line lab-welded sample prior to testing.	18
2.3	Lab-welded sample after application of artificial mud.	19
2.4	ACT 1 complete weekly programme	21
2.5	Samples in ACT1 covered with tray to prevent salt spray exposure. .	22
2.6	ACT 2 complete weekly programme	23
2.7	Samples in ACT2 at 45° angle	23
2.8	EXP 1 cycle	24
2.9	Boiling points of Aqueous MgCl_2 Solutions at One Atmosphere as a Function of Concentration	25
2.10	Geometry and dimensions of U-bend specimens specified by ASTM G36.	25
3.1	Split line weld of lab-welded samples of a) 304L and b) 301 after 6 weeks in ACT1 with $\text{NaCl}+\text{CaCl}_2$ mud mixture	28
3.2	Cross section of 304L lab-welded sample with $\text{NaCl}+\text{CaCl}_2$ mud mixture after 6 weeks in ACT 1.	28

3.3	Cross section of 304L lab-welded sample after 6 weeks in ACT1 with NaCl mud.	29
3.4	Cross section of 301 split line after 9 weeks in ACT 2	30
3.5	Flat samples a) 304L and b) 301 after 3 weeks in EXP1 chamber . . .	31
3.6	Sample from 304L split line weld after 9 weeks in EXP1 with NaCl + CaCl ₂ artificial mud.	31
3.7	U-bend specimen prior to ASTM stress corrosion cracking test	32
3.8	Results from initial ASTM G36 tests	33
3.9	U-bend samples after 16h in 34 wt % MgCl ₂ boiling at 146°C	33

1

Introduction

This chapter covers the motivation and background for this thesis work.

1.1 Stainless Steel Fuel Tank

Since the mid 1980s, automakers have been displacing coated-steel fuel tanks with plastic fuel tanks [1]. High-density polyethylene has traditionally been the resin of choice for plastic fuel tanks. Plastic tanks are very flexible when it comes to shape and complexity. The plastic tank can be made to fit whatever cavities are left by the vehicle design. However, stainless steel fuel tanks are also a viable option. The primary reason for this is to increase fuel volume. The increase in fuel volume is a result of decreasing the wall thickness when going from plastic to steel. Additionally, weight and emission losses are decreased. These factors make it worth investigating as a possible alternative to the plastic fuel tank.

Stainless steel has some drawbacks, however. It is difficult to form without breakage during stamping, more expensive, requires more steps to manufacture, and is susceptible to corrosion. Corrosion is hazardous as it can lead to fuel leakage and contamination of the fuel delivery system. Thus, proper steps must be taken to ensure that the fuel tank corrosion is minimized during its lifetime. The outside surfaces of the tank are exposed to road chemicals, salt, mud, and gravel. Gravel is a source of chipping, while the others are a source of chloride containing environments. The many welds used to join a steel fuel tank are particularly susceptible to

corrosion.

Another area of concern for fuel tanks is safety. Plastic fuel tanks are generally considered safer because they are seamless and therefore not prone to failures in seam areas. When a steel fuel tank absorbs energy and deforms, the pressure within the tank increases as the volume decreases. This makes welded areas vulnerable as they are typically areas of failure. The thermal properties of the tank material are also an issue. In North America the tank must withstand temperatures from -40°C to 79°C . Plastic fuel tanks must compensate for this by an increase in gauge thickness. This partially negates the weight savings.

Recently, a stainless steel fuel tank material and design have been developed that provides a reduction in weight compared to a plastic fuel tank with the same design [2]. The reduction in weight stems from the extremely thin walls of 1 mm and tailored strength that has excellent crash properties. The thin walls also provide an increase in fuel volume. However, many welds are present which is problematic for corrosion resistance. The corrosion resistance of these welds are the focus for this thesis investigation.

1.2 Scope of Work

The aim of this thesis is to assess the corrosion resistance of welds applied to austenitic stainless steel fuel tanks and develop a new test method for such welds. The primary material investigated is 301. The reference steel that is tested in parallel is 304L. Stress corrosion cracking (SCC) is of significant concern due to the susceptibility of austenitic stainless steel to this corrosion mechanism. Intergranular corrosion (IGC) is another likely corrosion process due to the relatively high carbon content of 301 compared to 304L. De-icing salts such as NaCl and CaCl₂ accelerate the corrosion process and are therefore essential to include in test cycles. Other important corrosion factors include temperature, relative humidity (RH), composition, and concentration of the chloride deposits.

1.3 Austenitic Stainless Steel

Austenitic stainless steels have a single-phase, face-centered cubic (fcc) structure that is maintained over a wide range of temperatures [4]. These steels typically have excellent formability, ductility, and toughness in the range from cryogenic temperatures up to 600°C. The FCC structure is primarily stabilized by nickel. Body centered cubic (BCC) stabilizers such as chromium and molybdenum must be carefully controlled in order to maintain the austenite phase. The standard austenitic steel grades can be divided into ASM 300-series (chromium-nickel alloys) and 200-series (chromium-manganese-nitrogen) stainless steels. The chromium content is necessary to control oxidation performance and thus corrosion resistance. The disadvantage of using austenitic stainless steels is their susceptibility to intergranular grain boundary corrosion and stress corrosion cracking. If the metal reaches the appropriate temperature range during heat treatment or welding, Chromium carbides precipitate at grain boundaries (sensitization) which leads to Cr depletion in adjacent regions. Naturally, this increases the rate of corrosion in these areas. Ti or Nb are added to stabilize carbon and prevent sensitization in higher grades (and

thus more expensive) of austenitic stainless steel. The steels used in this thesis work are 300 series austenitic stainless steels.

In general, austenitic stainless steels are considered the most weldable of the stainless steels. The thermal conductivity of austenitic steels is approximately half that of the ferritic steels. Consequently, the weld heat input required to achieve the same penetration is significantly reduced. However, the coefficient of thermal expansion (CTE) of austenite is 30 to 40% greater than that of ferrite, which results in increased distortion and residual stress during welding.

Austenitic stainless steel is susceptible to a number of corrosive attacks including:

- Intergranular corrosion (IGC)
- Preferential attack of weld metal precipitates
- Pitting and crevice corrosion
- Stress-corrosion cracking (SCC)
- Microbiologically induced corrosion

The work presented in this thesis concerns IGC and SCC. Pitting corrosion is discussed briefly as well, as it may provide initiation sites for SCC.

1.4 Influence of Alloying Elements on Corrosion Resistance

The different grades of stainless steel are produced by varying the amount and content of alloying elements [10]. This section provides a brief overview on the different alloying elements and their effect on alloy properties.

Chromium

Chromium is the most critical element pertaining to corrosion resistance in stainless steel. It is the element which promotes formation of the protective Cr_2O_3 layer. Once the Cr content has reached 10.5% an adherent surface film is formed that

prevents diffusion of oxygen into the surface and subsequent oxidation of the iron matrix.

Nickel

Nickel is the element most responsible for stabilizing the austenitic structure. It gives steel grades in the 300 series their strength, ductility, and toughness even at cryogenic temperatures. It does not help with formation of the passive layer.

Molybdenum

Molybdenum has a powerful effect on both generalized and localized corrosion resistance. Mo stabilizes the passive layer of Cr in chloride environments and helps reduce the initiation of pitting corrosion. As with Cr, the amount of Mo in stainless steel has a limit. A too high content of Mo promotes the formation of phases between 600°C and 900°C which are more susceptible to corrosion. The phases are enriched in Cr and Mo which makes them more noble than the surrounding matrix. This also depletes the amount of Cr and Mo in surrounding areas. Both of these effects result in an increased likelihood of corrosive attack. The precipitation formation is especially problematic in welds.

Nitrogen

Nitrogen is also an FCC stabilizer and increases resistance to pitting corrosion.

Carbon

Carbon is an essential element in stainless steel. It increases the strength and hardness of the alloy. A too high carbon content decreases corrosion resistance, however, due to the formation of chromium carbides. These carbides deplete the surrounding matrix of chromium that is needed to form the protective oxide layer.

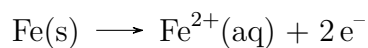
Titanium and Niobium

Ti and Ni are strong carbide formers and are often added to stabilize carbides. They will form preferentially to chromium carbide. This is especially useful for alloys that

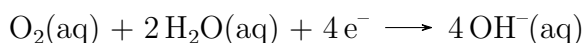
will be welded. However, these grades of steels are significantly more expensive.

1.5 Corrosion of Steels

Corrosion is an electrochemical process. It occurs through the operation of coupled electrochemical half-cell reactions. If electrons are products then the half-cell reaction is an oxidation reaction. If electrons are reactants then the reaction is a reduction reaction. The loss of metal is referred to as an anodic reaction. For example,



is an anodic reaction. It is anodic because Fe(s), the given species, undergoes oxidation and there is a loss of electrons at the anodic site. The electrons then travel to the cathode where a cathodic reaction takes place. In the case of corrosion in an aqueous solution, a common cathodic reaction is



In a cathodic reaction, a given species undergoes reduction, i.e. there is a decrease in oxidation number. There is also a gain of electrons at the cathodic site. On a corroding metal surface, anodic and cathodic reactions occur in a coupled manner at different locations on the metal surface [9].

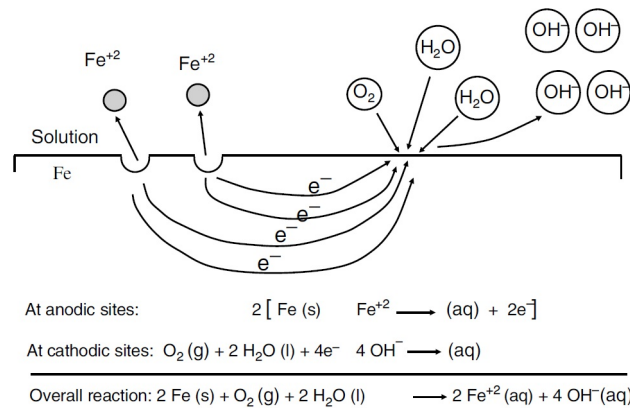


Figure 1.1: Coupled electrochemical reactions occurring at different sites on the same metal surface for iron in a neutral or basic solution

Figure 1.1 illustrates where the anodic and cathodic reactions take place for an iron surface exposed to a neutral or basic aqueous solution.

Four conditions are necessary in order for corrosion to occur. They are

1. An anodic reaction
2. A cathodic reaction
3. A metallic path of contact between anodic and cathodic sites
4. The presence of an electrolyte

An electrolyte is a solution which contains dissolved ions capable of conducting electrons. The most common electrolyte is an aqueous solution. A fuel tank will often be exposed to chloride containing aqueous solutions. In chloride containing aqueous solutions, the Cl^- ion acts as a catalyst.

There is a critical relative humidity necessary for corrosion to occur. This value is typically 50 - 70% for most metals. The critical relative humidity is the condition where multimolecular layers of water vapor physically absorb from the atmosphere onto the oxide-covered metal surface.

Stainless steel is a steel which contains at least 10.5% Cr by mass. At this amount, Cr reacts with oxygen and moisture in the environment to form a protective, adherent and coherent, oxide film that covers the entire surface of the material. The film is

often very thin, in the 2-3 nm thickness range. When the surface is damaged, i.e. from chipping or scraping, the surface self repairs as Cr rapidly reacts with oxygen and moisture in the environment.

1.6 Corrosion Mechanisms

The excellent corrosion resistance of austenitic stainless steel in most atmospheric environments is achieved by passivation of a thin (2 nm) layer of chromium oxide. Wet and humid chloride containing environments can facilitate several corrosion mechanisms in this material.

1.6.1 Pitting Corrosion

Pitting corrosion is common for stainless steels in chloride containing environments. Pitting corrosion is localized, accelerated dissolution of metal that occurs following breakdown of the otherwise protective passive oxide film [6]. Localized corrosion by pitting is difficult to detect since the diameter of the pit is small, weight loss is negligible, and corrosion products on the surface may cover pits. As such, pitting corrosion is dangerous and can cause unexpected catastrophic failure. In the presence of applied stress, pits can serve as initiation sites for stress corrosion cracking, which will be discussed in the next section. Pitting is caused by the presence of an aggressive anion in the electrolyte, usually Cl⁻ since it is so common in the atmosphere. The chloride ion is a strong electron donor and tends to interact with electron acceptors, such as metal cations. Additionally, the chloride ion is relatively small and has high diffusivity [9].

The tendency of a metal to undergo pitting is characterized by its critical pitting potential. In the absence of chloride ions, the metal remains passive up to the electrode potential of oxygen evolution. However, in the presence of chloride ions, the passive film suffers local attack. In this case, pitting initiates at a well-defined po-

tential called the critical pitting potential. Once initiated, corrosion pits propagate rapidly, as shown by the sharp increase in current density at electrode potentials just beyond the critical pitting potential. The critical pitting potential, E_{pit} , is a characteristic property of a given metal or alloy and the value depends on chloride concentration. For a given chloride concentration, the more positive E_{pit} , the more resistant the metal is to pit initiation. Chloride ions initiate pitting. The E_{pit} decreases as chloride concentration increases.

During welding, microstructural and surface changes take place which make it impossible to predict the corrosion resistance by a single expression [5]. Reworks, i.e. grinding to remove surface oxides may also decrease corrosion resistance if not done properly.

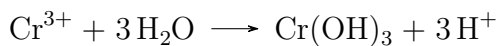
1.6.2 Stress Corrosion Cracking (SCC)

The following are several important characteristics of SCC:

- A tensile stress is required. The tensile stress may be external, but in the case of a fuel tank, welding introduces residual stress.
- Metals or alloys which experience SCC usually have good resistance to general corrosion. For examples, stainless steel is usually very resistant to general corrosion in neutral solutions, but is prone to SCC
- Specific environments cause SCC in certain alloys. For example, Cl⁻ environments cause SCC in stainless steel. This environment is typically encountered in driving conditions.

Residual tensile stress accumulates in the weldment from thermal cycling during welding. Stress levels in this region can approach the yield strength of the base metal. If the threshold stress is exceeded and the weld is exposed to a chloride containing environment, SCC is likely to occur.

The two primary stages of SCC are initiation and propagation. During initiation, mechanical damage or chemical attack by aggressive ions causes localized breakdown of the protective oxide layer [9]. The exposed base metal leads to formation of a corrosion pit and subsequent initiation and propagation of a stress-corrosion crack. The corrosion pit is a stress intensifier. Local stress is amplified near the corrosion pit. The corrosion pit is also a source of H⁺ ions. For stainless steel, the following reaction within a corrosion pit



generates H⁺ ions at the tip of an emerging stress corrosion crack. This reaction can also occur with propagating stress corrosion cracks.

During propagation, the electrolyte within the crack becomes acidic due to the hydrolysis of dissolved metal cations. The stress corrosion cracks propagate and grow due to the combined effects of the residual stress and the corrosive conditions within the crack tip. Once propagation begins, the crack path may be intergranular or transgranular. Intergranular cracks grow along grain boundaries while transgranular cracks travel across grain boundaries. The concentration of the electrolyte influences crack growth behaviour. In general, an increase in concentration of the aggressive ion causes an increase in SCC susceptibility. An increase in temperature also increases the susceptibility to SCC and increase in crack growth rate.

Cracking is typically characterized by crack branching. Increasing the ferrite content in stainless steel weld metals reduces SCC susceptibility. If the welding parameters are not optimized then a postweld heat treatment must be performed to reduce the magnitude of residual tensile stress. The heat input during welding directly affects the amount and distribution of residual stress. The welding process produces very localized strains which lead to distortion and residual stress.

The tendency of austenitic stainless steels to undergo atmospheric SCC increases

with increasing temperature, decreasing alloying level, and decreasing relative humidity (RH), for RH values above the deliquescence point of a given salt [8]. Deliquescence is the process by which a substance absorbs moisture from the atmosphere until it dissolves in the absorbed water and forms a solution. It has been proposed that the equilibrium chloride concentration in the surface electrolyte formed as a result of the interaction of chloride salt and water vapor in air governs the initiation of SCC [8]. Chloride concentration decreases with increasing RH as the solution absorbs more water from the air and the volume of the solution increases.

1.6.3 Intergranular Corrosion

Intergranular corrosion is the result of sensitization. Thermal cycling causes carbon to diffuse to austenite grain boundaries and form chromium carbides, thus depleting chromium from regions adjacent to grain boundaries. This chromium depletion produces very localized galvanic cells. This type of corrosion typically occurs in the HAZ. Once the Cr content dips below 12%, intergranular attack may occur.

At temperatures above 1035°C, Cr carbides are completely dissolved in austenitic stainless steels. However, when these steels are slowly cooled or reheated from 425 to 815°C, Cr carbides are precipitated at grain boundaries. Once sensitization occurs, the depleted zones have a higher corrosion rate than the surrounding region. If the steel is rapidly cooled below 425°C then carbides do not precipitate and IGC will not occur.

The time-temperature-sensitization diagram in Figure 1.2 details the formation of Cr carbides necessary to cause sensitization. The diagram shows susceptibility to sensitization as a function of time, temperature, and carbon content.

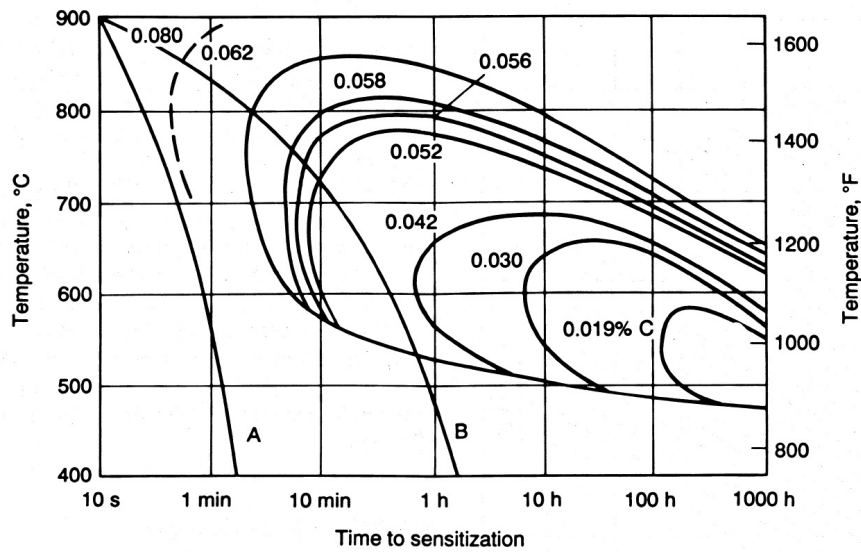


Figure 1.2: Time-temperature-sensitization curves for type 304 stainless steel in a mixture of CuSO_4 and HSO_4 containing copper. Source: Ref 14. Curves A and B indicate high and medium cooling rates, respectively

If the cooling rate is sufficiently rapid then the cooling curve will not intersect the C-shaped curve necessary for Cr carbide formation. At sufficiently low cooling rates, the cooling curve eventually intersects the C-shape curve, indicating that sensitization will occur.

The control of stainless steel sensitization may be achieved by using:

- A postweld anneal and quench to redissolve the chromium at grain boundaries
- A stainless steel with low carbon (e.g. 304L or 316L) to avoid carbide formation
- A stabilized grade of stainless steel, containing Ti and/or Nb, which preferentially form carbides and leave chromium in solution

Welding parameters must be carefully considered to reduce the risk of these corrosion mechanisms being active. Excessive high heat input will aid in the development of both SCC and IGC.

1.7 The Effect of Welding on Corrosion

Welding is a technique used to join metallic parts through the application of heat. During this process, the arc is shielded by an inert gas such as argon or helium. [3]. The welding process involves repeated thermal cycling and thus microstructural changes to the weld metal. These changes can be significant, and detrimental to corrosion resistance if the welding parameters are not carefully controlled. Welding parameters influence the amount and distribution of residual stress [4]. The heat input directly effects the size of the weld deposit. Small weld deposits are advantageous because they reduce residual stress and the possibility of cracking. In addition to residual stress, other metallurgical factors include:

- Precipitation of secondary phases
- Recrystallization and grain growth in the heat affected zone (HAZ)
- Volatilization of alloying elements from the molten weld pool
- Contamination of the solidifying weld pool

Corrosion resistance can usually be maintained in the weld by balancing alloy composition to limit unfavorable precipitation reactions, by properly shielding the molten weld pool from the surrounding environment, by removing Cr-enriched oxides and Cr-depleted base metal from heat tinted surfaces, and by choosing proper welding parameters [4]. The difficulty of welding stainless steel is primarily due to the high carbon content of the base metal in additiona to the high residual stresses incurred by welding. These factors lead to intergranular corrosion (IGC) and stress corrosion cracking (SCC), respectively.

Weld Oxides

Surface oxides are formed when molten metal is exposed to oxygen in the atmosphere. These oxides cause visible discoloration of the metal surface - referred to as "heat tint". The formation of surface oxides during welding can reduce corrosion resistance in chloride containing environments [5]. The reduced corrosion resistance is related to the oxide properties, including:

- Chemical composition
- Non-homogenous structure
- Depletion of alloying elements from base material

Above temperatures of approximately 450°C, the formation of oxides can have a deleterious impact on corrosion resistance. Thus, the thermal cycling and oxide content of the surrounding environment must be controlled in order to reduce harmful oxidation during welding. Both the surface being welded and the root side must be properly shielded to minimize oxidation. The root side is opposite of the side being welded. This side also reaches temperatures high enough for oxides to form. If not properly shielded, the surface oxides must be removed using an appropriate post weld cleaning method.

1.8 The Role of Ferrite Content

During welding of austenitic stainless steel, a high temperature phase of ferrite, known as delta ferrite, may be formed. The ferrite content influences the susceptibility for solidification cracks in the weld metal and corrosion resistance. Typically a ferrite content of approximately 3-11V% is desired. At this level, delta ferrite prevents initiation of fracture during weld solidification and microcracking [4]. Delta ferrite can also provide resistance to SCC in chloride environments, as it impedes crack propagation through the austenite phase. Delta ferrite raises the yield point of austenitic welds, particularly those alloys with low carbon and nitrogen content. Increasing the yield strength and resistance to SCC is related to the higher yield point of delta ferrite than of austenite. The morphology of delta ferrite is impor-

tant as well. If the ferrite content is too high, continuous networks of ferrite may form. This may be harmful for SCC as it provides a continuous path for crack propagation [7]. However, delta ferrite has little to no effect on IGC and pitting corrosion.

The Schaeffler diagram is a useful tool for estimating the microstructure of a steel with a given chromium and nickel equivalent that is rapidly cooled from 1050°C to room temperature. The nickel equivalent (Ni)eq is the sum of all the fcc stabilizers and the chromium equivalent (Cr)eq is the sum of all chromium stabilizers.

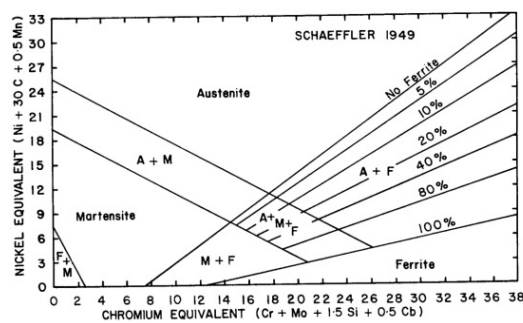


Figure 1.3: Schaeffler diagram for estimating steel microstructure

This diagram will later be used to calculate the approximate ferrite content of the stainless steels studied for this thesis.

2

Materials and Methods

In this chapter the experimental setup and test methods will be discussed. Welded laboratory prepared samples were used to assess weld corrosion behaviour when exposed to different accelerated corrosion tests.

Two different types of austenitic stainless steels from Outokumpu, 304L and 301, were investigated. The chemical compositions for these steels are listed in Table 2.1.

		AISI 301	AISI 304L
Chemical Composition (wt%)	Cr	18.20	18.20
	Ni	7.20	8.10
	Mo	0.07	-
	C	0.060	0.022
	Si	0.32	0.38
	P	0.026	0.034
	S	0.0010	0.0020
	N	0.101	0.048
	Nb	0.003	-

Figure 2.1: Chemical compositions of stainless steels 301 and 304L.

The samples from Outokumpu were lab-welded with TIG and all had the same size, thickness, geometry, and welding parameters. A sample prior to exposure are shown below in Figure 2.2. Samples were approximately 6 cm in length and 4 cm in height.

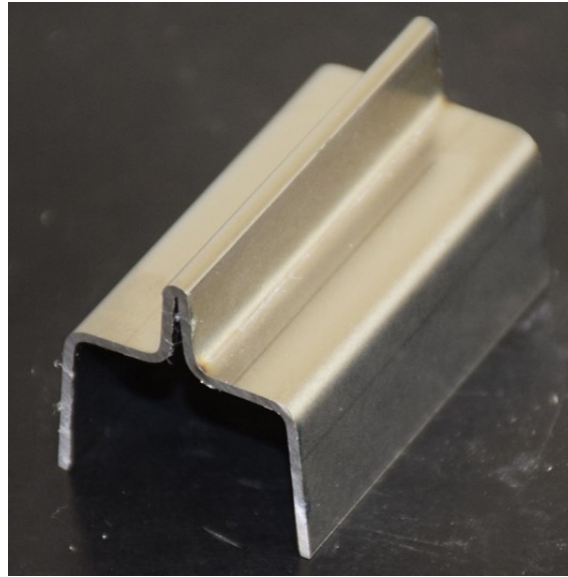


Figure 2.2: Split line lab-welded sample prior to testing.

The only difference between the two lab-welded stainless steels is their composition. The primary difference in composition is carbon content. The 301 contains about 0.06%C whereas 304L has 0.03%. The samples received from Outokumpu were specifically designed and welded for corrosion testing. As such, these samples were prepared under optimal conditions and welding parameters.

All samples were degreased with ethanol prior to testing. After testing, cross sections were prepared for metallographic investigation. Cross sections were generally prepared where corrosion appeared to be worst. These samples were ground to P 4000 and polished with 1 μm diamond paste. Light optical microscopy (LOM) was used for all microscopic analysis.

2.1 Artificial Mud

Artificial mud was applied to samples for two of the accelerated corrosion tests (described below). The purpose of the mud is to simulate what a car component might be exposed to during real driving conditions. The mud combines sand, kaolin (clay) to form a paste, and salt to mimic actual mud and road dirt. Two different artificial

mud mixtures were prepared according to the Volvo Cars "Test of Pitting Corrosion resistance, method ID 005104/1". One batch of mud was prepared with a 2.5 wt % NaCl and the other with a 2.25 wt % NaCl + 0.3 wt % CaCl₂.

The mud was applied in a manner such that it formed a thin, adherent film on the sample surface. The mud covered the split line weld fusion zone, HAZ, and a portion of the base metal. A sample covered in mud, prior to testing, is shown below in Figure 2.3.

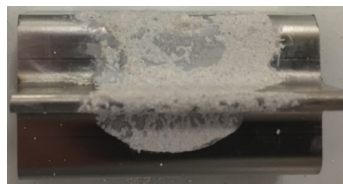


Figure 2.3: Lab-welded sample after application of artificial mud.

2.2 Climate Chamber Tests

Samples of both 304L and 301 lab-welded samples were used for climate chamber corrosion testing. Three climate chambers were used to perform different accelerated corrosion cycles. The corrosion tests were selected to simulate various conditions. These exposures included two Volvo Cars standard accelerated corrosion tests (ACT). These two different cycles are referred to as ACT1 and ACT2. The specific parameters for the ACT cycles are detailed below. A third, experimental cycle (EXP1) was also included. The EXP1 is a lower temperature cycle that ranges from 5°C to 20 °C. The ACT 1 and ACT 2 were chosen because they are standard tests that Volvo Cars uses to assess corrosion performance. EXP1 was used to see if corrosion would occur in a lower temperature range with constant dew point throughout testing. Duplicate sets of samples were exposed for 6 weeks and 9 weeks in each chamber. All samples tested in ACT1 and EXP1 had artificial mud applied. These samples were also re-mudded every 3 weeks.

2. Materials and Methods

The list of samples and conditions tested are as follows:

Lab-welded Samples:

- ACT1, 301 and 304L, 3, 6, and 9 weeks, NaCl and NaCl+CaCl₂ mud
- ACT2, 301 and 304L, 3, 6, and 9 weeks
- EXP1, 301 and 304L, 3, 6, and 9 weeks, NaCl and NaCl+CaCl₂ mud

2.3 ACT 1

ACT 1 follows a 12h temperature, humidity cycle according to VCS 1027, 149 [16]. While not shown in 2.4, there is also a twice weekly automated salt spray. Mud was applied to the surface of all samples tested in ACT1. The samples were covered to protect from the salt spray cycle. This was done because the mud on the samples contained a known chloride composition. The salt spray cycle would have altered this composition.

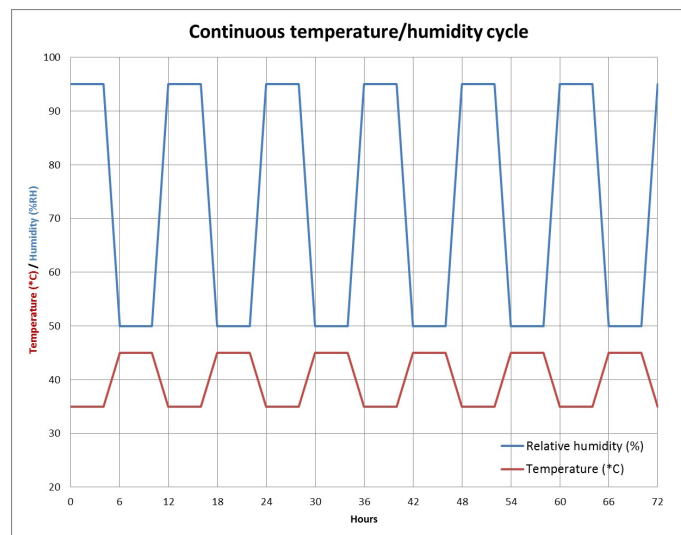


Figure 2.4: ACT 1 complete weekly programme

According to Figure 2.4 the cycle follows 4h at 35°C, 95% RH, 2h linear transition to 4h at 45°C, 50% RH and 2h linear transition back to 35°C, 95% RH.

The sample positioning in the chamber is shown in Figure 2.5



Figure 2.5: Samples in ACT1 covered with tray to prevent salt spray exposure.

This simple set up prevents exposure to the salt spray while not altering the exposure environment.

2.4 ACT 2

ACT 2 is a laboratory-accelerated atmospheric test. The workday test procedure consists of:

A 6h wet phase at room temperature, with intermittent exposure to salt solution (0.5% NaCl). A 2.5h transition phase with drying under climate control A 15.5h phase with constant temperature and humidity (50°C, 70% RH). The procedure is repeated Mon-Fri followed by a 48h weekend phase under constant climate control (50°C, 70% RH). A graph detailing the complete weekly cycle is shown below in Figure 2.6.

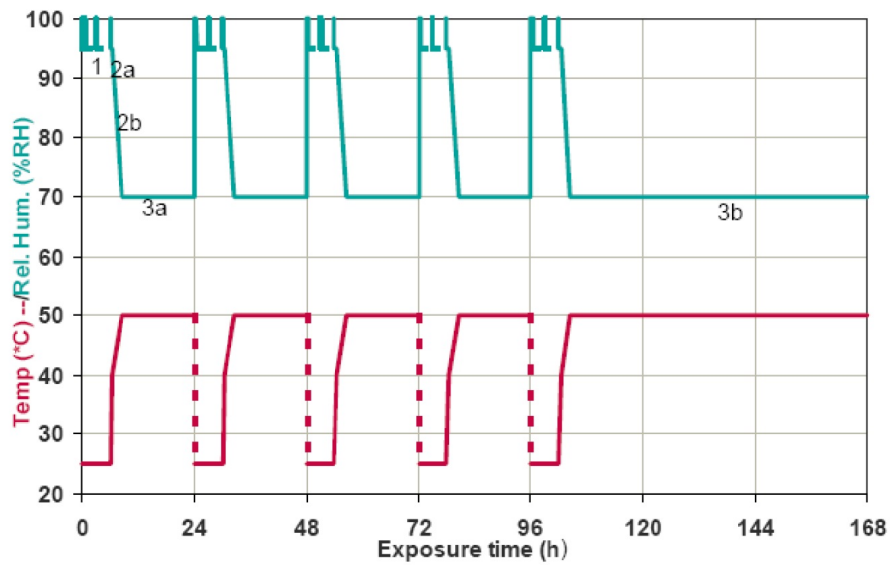


Figure 2.6: ACT 2 complete weekly programme

During this cycle, samples are completely exposed to the environment and no artificial mud is applied. The samples are placed at roughly a 45 °angle to prevent salt spray from stagnating on the surface as seen in Figure 2.8



Figure 2.7: Samples in ACT2 at 45°angle

2.5 EXP 1

The Experimental 1 (EXP1) cycle ranges from 5°C to 20°C. The temperature cycle is programmed with the relative humidity to maintain the same dew point throughout testing.

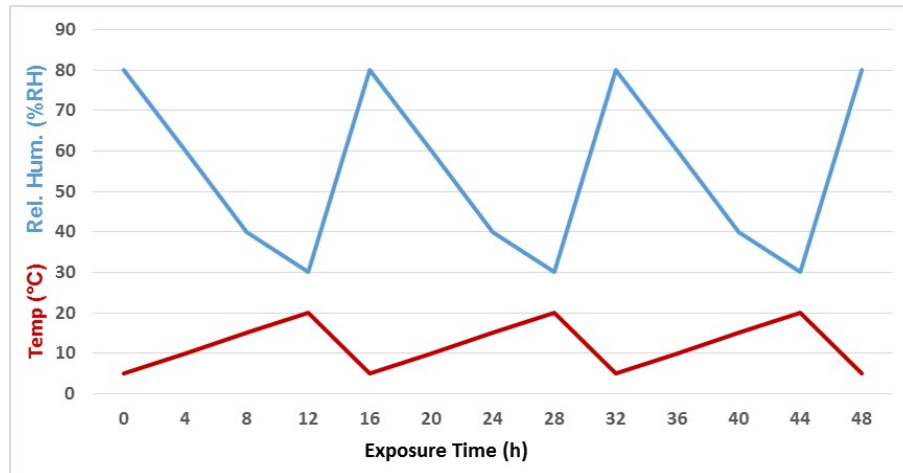


Figure 2.8: EXP 1 cycle

The maximum temperature of 20°C for this cycle is much lower than the maximum temperature of 45°C for ACT 1 and 50°C for ACT 2. This cycle was included to see if corrosion would still occur at this lower temperature and to compare it to ACT1 and ACT2.

2.6 ASTM Test for Stress Corrosion Cracking

In addition to the accelerated corrosion test cycles, an ASTM "Standard Practice for Evaluating Stress-Corrosion-Cracking Resistance of Metals and Alloys in a Boiling Magnesium Chloride Solution" was also used [18]. This test was performed at both Volvo Cars and Outokumpu, the material supplier. This test provides a rapid method for ranking the relative degree of SCC susceptibility for stainless steels and related alloys in aqueous chloride-containing environments. The procedure recommends to use a $MgCl_2$ solution that boils at 155°C. This correlates to approximately

45 wt % MgCl_2 as seen below.

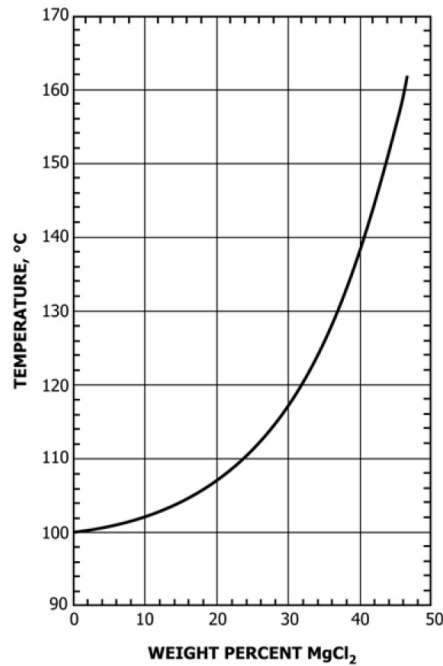


Figure 2.9: Boiling points of Aqueous MgCl_2 Solutions at One Atmosphere as a Function of Concentration

However, this composition was determined to be too high for austenitic stainless steel. Tests were instead performed at 12%, 20%, 30% and 34% MgCl_2 . U-bend specimens were used according to the standard specifications shown in 2.10. After bending, samples were placed in the solution and periodically checked until cracks on the surface were noticeable.

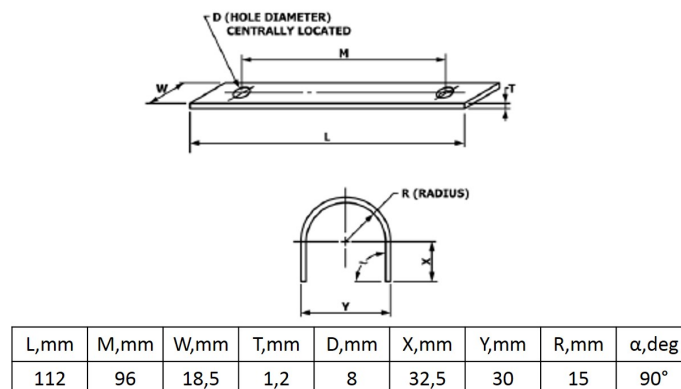


Figure 2.10: Geometry and dimensions of U-bend specimens specified by ASTM G36.

3

Results and Discussion

In the following chapter, the results of the accelerated corrosion tests are given and discussed.

3.1 Laboratory Climate Chamber Tests

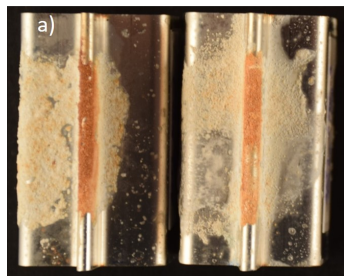
Initially, climate chamber tests were intended to run for 3 weeks and 6 weeks. However, after 3 weeks there was no observable corrosion on the surface of any sample. The sample exposures were then extended to 6 and 9 weeks.

3.1.1 ACT 1

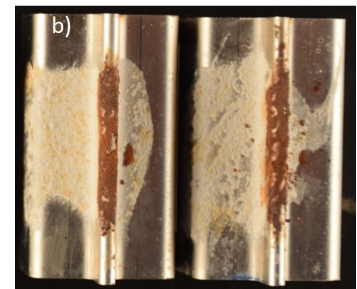
3.1.1.1 Lab-welded Samples

Following 6 weeks of exposure in ACT 1, lab-welded samples showed only very slight signs of corrosion. Two samples prior to mud removal are shown in Figure 3.1.

3. Results and Discussion



(a)



(b)

Figure 3.1: Split line weld of lab-welded samples of a) 304L and b) 301 after 6 weeks in ACT1 with NaCl+CaCl₂ mud mixture

On each sample a dark brown discoloration is formed along the weld seam. Clearly the mud on 301 in 3.1a is darker than on the 304L in 3.1b. However, this does not appear to correlate with the extent of corrosion. Upon mud removal, only some minor pitting on the surface was observed under the microscope. Cross sections from these samples as well as samples with NaCl mud were prepared. Several small pits of 20-60 μm were observed along the surface of the fusion zone, as shown in Figures 3.2 and 3.3. No SCC or IGC was observed in the cross section.

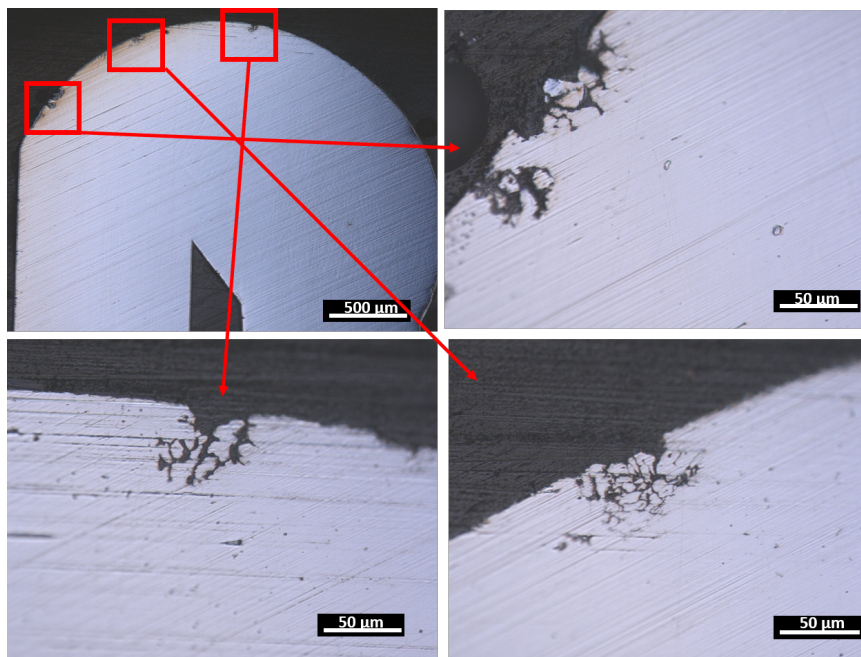


Figure 3.2: Cross section of 304L lab-welded sample with NaCl+CaCl₂ mud mixture after 6 weeks in ACT 1.

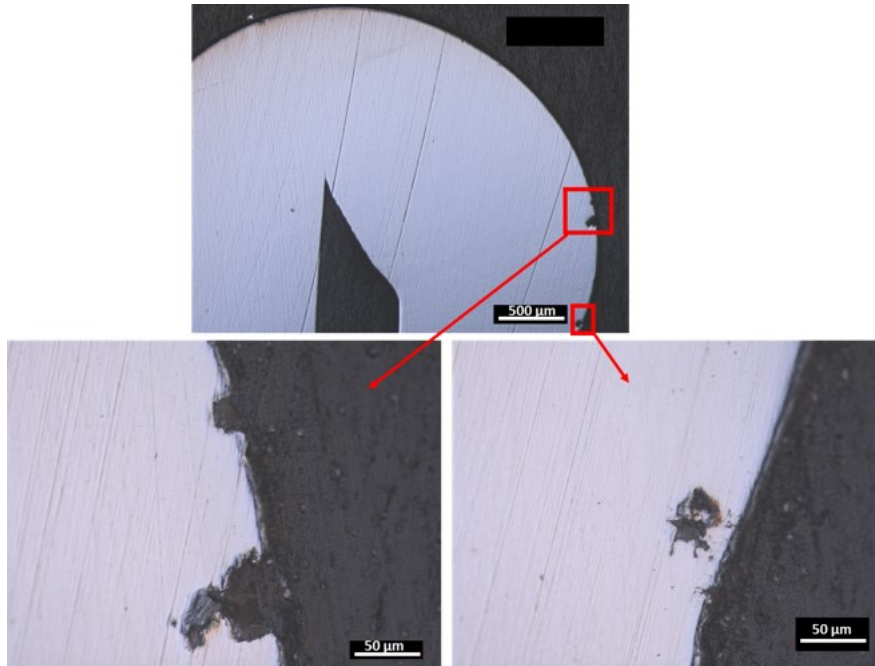


Figure 3.3: Cross section of 304L lab-welded sample after 6 weeks in ACT1 with NaCl mud.

Samples from Figures 3.2 and 3.3 had the most severe, corrosion that occurred in any lab-welded sample exposed to ACT 1 after 6 weeks. However, this corrosion was still very minimal and much less than expected based on the relatively high salt content. Samples after 9 weeks were similarly unaffected. Again, 304L showed some very minor pitting on cross sections but no additional corrosion was observed.

3.1.2 ACT 2

3.1.2.1 Lab-welded Samples

Following 6 and 9 weeks of exposure in ACT 2, Outokumpu lab-welded samples showed almost no sign of corrosion. As with ACT1 samples, some slight corrosion products were seen on the surface. There was some minor pitting in the weld zone and heat affected zone (HAZ). The base metal was completely unaffected. All of the cross sections had the same appearance as in Figure 3.4.

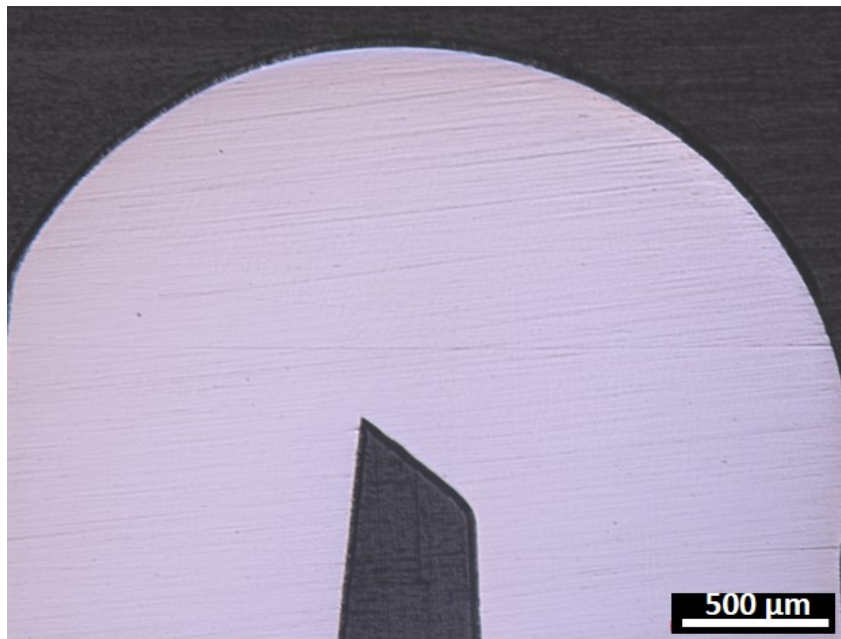


Figure 3.4: Cross section of 301 split line after 9 weeks in ACT 2

This figure looks the same as that of an as-received cross section prior to testing. This is how most of the lab-welded cross sections appeared after both ACT1 and ACT2. The excellent weld quality makes it difficult for corrosion to occur, even after 9 weeks.

3.1.3 EXP 1

Prior to arrival of the welded samples from Outokumpu, flat samples of 304L and 301 were tested with artificial mud in EXP 1. The samples were exposed for 6 weeks total and examined after 3, 4, 5, and 6 weeks. Two different artificial muds were used, one with 2.5% NaCl and one with 2.5% CaCl₂. The results of this test after 3 weeks are shown below in Figure 3.5.

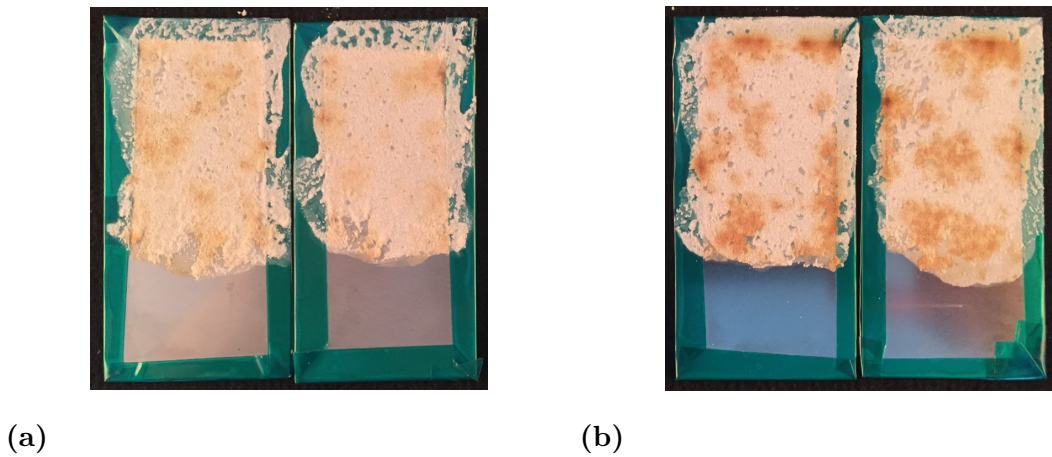


Figure 3.5: Flat samples a) 304L and b) 301 after 3 weeks in EXP1 chamber

Again, the discoloration of the mud on the surface does not indicate that corrosion has occurred. Even after 6 weeks with the more aggressive CaCl_2 mud there was no pitting observed. A similar test performed at Outokumpu on the same material showed that no pitting corrosion occurred below 20°C .

Outokumpu lab-welded samples were also tested in this cycle. It was thought that the welds could facilitate corrosion. However, this was not the case. No sample showed any signs of corrosion on the surface or cross section following 6 weeks and 9 weeks of exposure. A cross section from one of the samples is shown in 3.6.

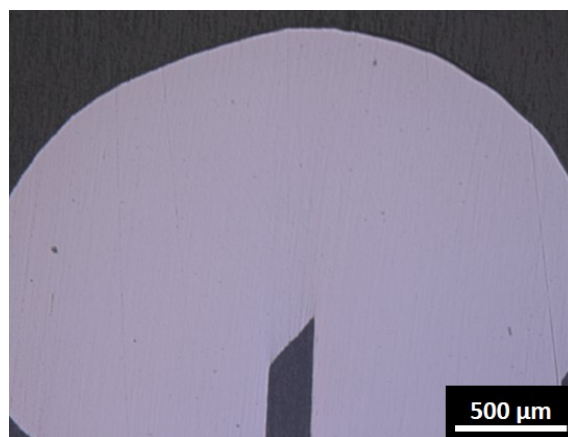


Figure 3.6: Sample from 304L split line weld after 9 weeks in EXP1 with $\text{NaCl} + \text{CaCl}_2$ artificial mud.

This result indicates that the cycle is not aggressive enough to cause corrosion in

any reasonable time frame for these samples.

3.2 ASTM Stress Corrosion Cracking

The majority of the experimental and analysis work for ASTM G36 was recently performed at Outokumpu. They have experience with this test as well as the proper chemical setup. However, this test was also attempted at Volvo Cars using the lab-welded specimens from Figure 2.2. Only one test was performed using 12% MgCl_2 . The test was stopped after 10 days and no cracks were observed on the surface or cross section. The concentration was determined to be too low to induce SCC in this time frame.

The tests at Outokumpu used flat samples that were first bent into a U shape prior to testing. This was done to follow the standard specifications as closely as possible. The bending introduces a high level of stress in the material. A sample prior to testing is shown in Figure 3.7

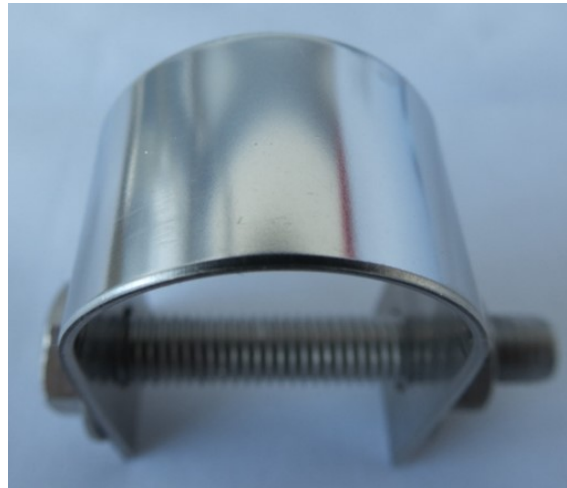


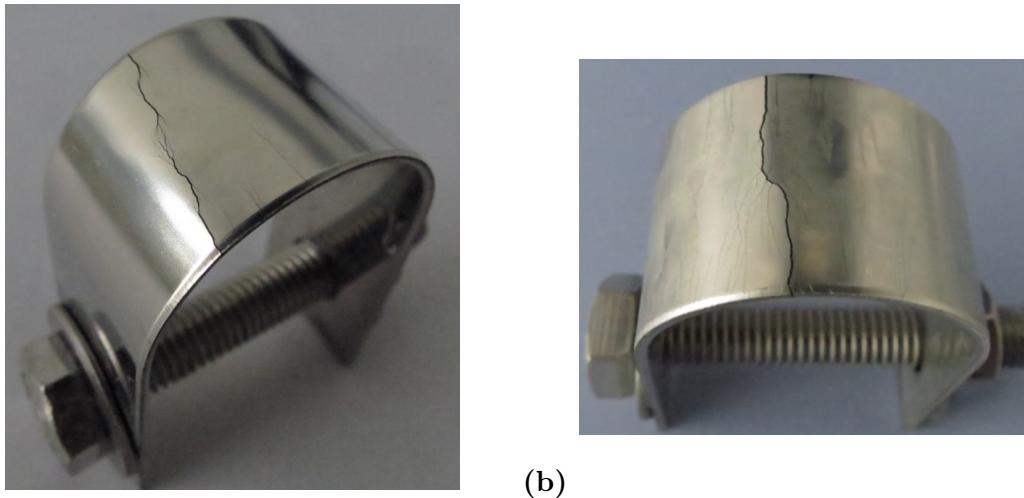
Figure 3.7: U-bend specimen prior to ASTM stress corrosion cracking test

Tests were performed on both 304L and 301. Results showed that the two grades perform similarly in the different concentrations of MgCl_2 . The results of tests thus far are shown in Figure 3.8

Condition	Duration	301	304L
25% NaCl	600h+	0/3 fail	0/3 fail
20% MgCl ₂	260h	0/3 fail	0/3 fail
30% MgCl ₂	145h	2/2 fail	1/2 fail
34% MgCl ₂	16h	3/3 fail	3/3 fail

Figure 3.8: Results from initial ASTM G36 tests

The first condition listed in Figure 3.8, 25 wt % NaCl, is from a similar ASTM standard for SCC that uses boiling NaCl instead of MgCl₂. Clearly, the duration to failure is much longer than for MgCl₂. The criteria for "fail" is the appearance of cracks on the surface as in Figure 3.9



(a)

(b)

Figure 3.9: U-bend samples after 16h in 34 wt % MgCl₂ boiling at 146°C

The aim of this test is to compare the SCC resistance of 301 and 304L. It is important to emphasize that the purpose of this test is to induce cracking. The formation of cracks without additional context does not indicate quality of the material. The duration must also be taken account. Since this test is still in its early stages, the sample size is quite small. Thus far, only 3 samples of each 304L and 301 have been

3. Results and Discussion

tested for each condition. However, these early results are very promising for several reasons. Figure 3.8 shows that the rate of failure is nearly the same for 304L and 301. The results also show that this standard could be quite useful for testing welded austenitic stainless steel at Volvo Cars. The primary advantage is the significantly shorter duration of testing. However, this standard is only a general test for SCC and is not linked to any specific application. Many iterations of this test must be performed to before incorporating it into a test procedure for austenitic stainless steel welds.

4

Conclusion

The results did not show a clear difference between 301 and 304L lab-welded samples. Weld parameters were optimized in such a way to minimize sensitization and residual stress. In such a case, the elevated carbon content of 301 has less influence on corrosion behaviour. It is beneficial to know that the materials themselves are very corrosion resistant even in the aggressive ACT cycles.

On the other extreme, the experimental cycle is not aggressive enough with the low temperature range from 5°C to 20°C for the specific samples tested in this work. Additional experimental tests should be run to determine an appropriate temperature and humidity cycle for corrosion to occur. The long duration (at least 6 weeks) of testing make it difficult to determine appropriate climate conditions. This is why it would be extremely beneficial to implement ASTM standard corrosion tests for SCC and IGC.

Results from the ASTM G36 test indicate that this standard could be useful for testing of welded austenitic stainless steel at Volvo Cars. The duration of testing is much shorter than the ACT cycles. This is only a general test for SCC and is not linked to any specific application. As such, more iterations of this must be performed to adapt the standard to welded stainless steel. Studies must also be done to correlate these results to real driving conditions.

4. Conclusion

5

Outlook

More climate chamber accelerated corrosion tests need to be performed to determine appropriate parameters for testing austenitic stainless steel welds. A test should be developed that can be used to signify a pass or fail after 6 weeks, or less, of exposure. The EXP1 cycle was a step in this direction but the temperature was too low. Future work should focus on the 30 °C to 40 °C range. Some tests should also be run with higher CaCl₂ concentration to see how this influences weld corrosion.

If stainless steel fuel tanks become used in future cars then more research could be performed to qualify ASTM standards for this specific application. In addition to ASTM G36 for stress corrosion cracking there is also ASTM A262 for detecting susceptibility to intergranular corrosion. These tests could also be used as pass or fail criteria. For example, if no SCC or IGC is present after a specified duration then the weld quality is passable. The primary advantage of these standards is that they are rapid in comparison to ACT1 and ACT2.

Lastly, more work should be done to assess the effect of weld quality on corrosion behaviour. This study has shown that lab-welded samples are extremely corrosion resistant in the ACT cycles. However, the quality of welds on the real fuel tank will not be the same as those of the laboratory prepared samples.

Bibliography

- [1] Alvarado, P.J. (1996) Steel vs. plastics: The competition for light-vehicle fuel tanks. pp. 22-25. JOM
- [2] Outokumpu's stainless steel makes fuel tank lighter and safer (2014)
- [3] Welding Metallurgy. Encyclopedia Britannica. Online
- [4] Davis, J.R. (2006) Corrosion of Weldments. ASM International
- [5] Lars Ödegård. (1996) Welding of stainless steels corrosion in welds: effect of oxides, slag and weld defects on the pitting resistance. Vol. 43 Issue: 4. pp.11-17. Anti-Corrosion Methods and Materials.
- [6] G.S.Frankel, N.Sridhar. (2008) Understanding localized corrosion. Vol. 11 Issue: 10. pp. 38-44. Materials Today.
- [7] H.S. Khatak. (2002) Corrosion of Austenitic Stainless Steels: Mechanism, Mitigation and Monitoring. Woodhead Publishing.
- [8] Prošek, Tomáš and Thierry, D. (2014) Low-Temperature Stress Corrosion Cracking of Austenitic and Duplex Stainless Steels Under Chloride Deposits. Vol. 70. Corrosion.
- [9] McCafferty, E. (2010) Introduction to Corrosion Science. Springer New York
- [10] The effects of alloying elements. [Online]
- [11] The stainless steel family. International Stainless Steel Forum. [Online]
- [12] T Wegrzyn. (1992) Delta ferrite in stainless steel weld metals. pp. 690-694. Welding International.
- [13] J.R. Davis. (1994).ASM Specialty Handbook: Stainless Steels. ASM International.

- [14] T. Von Molkte. (1992) The Influence of Heat-tinted surface layers on the corrosion resistance of stainless steels. Vol. 2. pp. 185-195. Proceedings of the 1st International Chromium Steel and Alloy Congress.
- [15] Michael F. McGuire. (2008) Stainless Steels for Design Engineers. ASM International.
- [16] "Test of Pitting Corrosion resistance". Method ID 005104/1.
- [17] Accelerated corrosion test – ACT II. VCS 1027/1449.
- [18] ASTM G36. (2013) Standard Practice for Evaluating Stress-Corrosion-Cracking Resistance of Metals and Alloys in a Boiling Magnesium Chloride Solution.